HEFAT2012
9th International Conference on Heat Transfer, Fluid Mechanics and Thermodynamics
16 – 18 July 2012
Malta

DROP FORMING REGIMES IN VISCOUS CO-FLOWING LIQUID-LIQUID-SYSTEMS WITH EQUAL DENSITY

Sellerberg, M.*, Szemplinski, B. and Walzel, P.
*Author for correspondence
Department of Biochemical and Chemical Engineering
Mechanical Process Engineering,
TU Dortmund,
Dortmund,
Germany,
E-mail: monika.sellerberg@bci.tu-dortmund.de

ABSTRACT

Drop formation at orifices and capillaries is applied in different industrial applications. The transition from dripping to the laminar jetting regimes must be known. In the non-viscous case the transition point is characterized by a transitional Weber number $We = 2$. For the viscous case particularly considered here, another characteristic number is maybe more suitable. Experiments are performed with viscous liquids for both phases with equal density to obtain the characteristic parameter for the transition. Droplet diameter, break up length and distance of droplets which refers to the break up wavelength in the jetting regime are analysed. In the laminar jetting regime different kinds of drop formation could be observed and the influence of the volumetric flow rate ratio to the jet diameter and relaxation length is reported as well.

INTRODUCTION

When a low viscous liquid is injected via a capillary into a second immiscible but stagnant liquid, four different phenomena can be observed, as it is shown in Figure 1. At low velocities of the disperse phase droplets are formed directly at the capillary. This is called dripping mode (Figure 1 A). By increasing the velocity a liquid thread is formed first. Due to surface tension axisymmetric disturbances grow and the jet finally breaks up into droplets (Figure 1 B). The laminar jetting region is followed by the turbulent jetting region when the discharge velocity is further increased (Figure 1 C). The disturbance is no longer axisymmetric and the whole thread is distorted. The last phenomenon is spraying (Figure 1 D). At high discharge velocity the liquid is then dispersed directly at the capillary tip into droplets with a wide droplet size distribution. In this paper the dripping and laminar jetting mode is further described and analysed.

NOMENCLATURE

a	[m]	Edge length of the channel
Ca	[-]	Capillary number (= $u\,\mu_D / \gamma$)
d'	[m]	Theoretical jet diameter
d	[m]	Diameter
D	[m]	Tube diameter
F	[-]	Harkins-Brown correction factor
g	[m/s²]	Gravitational acceleration
H	[m]	Channel height
K	[-]	Parameter
L	[m]	Length
u'	[m/s]	Velocity at phase interface
u	[m/s]	Velocity
V	[m³]	Volume
We	[-]	Weber number (= $\rho_D\, u^2_{D\,dc,I} / \gamma$)

Special characters

α	[-]	Viscosity ratio (= μ_D / μ_C)
γ	[N/m]	Interfacial tension
λ	[m]	Wavelength
μ	[Pas]	Viscoity
φ	[-]	Disperse phase fraction
ρ	[kg/m³]	Density
$\Delta\rho$	[kg/m³]	Density difference

Subscripts

B	Breakup
c	Capillary
C	Continuous phase
$crit$	Critical
d	Droplet
D	Disperse phase
$Dripping$	Dripping regime
i	Inner
J	Jet
$Jetting$	Jetting regime
o	Outer
R	Rayleigh
$relaxation$	Relaxation

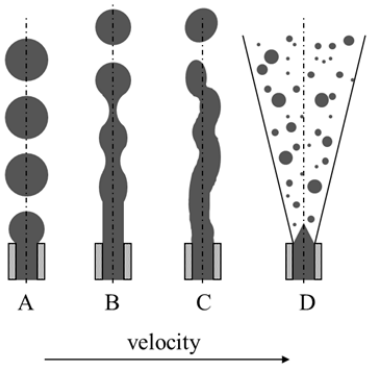

Figure 1 Drop formation regimes; A: dripping, B: laminar jetting, C: turbulent jetting and D: spraying

TRANSITION BETWEEN DRIPPING AND JETTING

The breakup of low viscous liquids in gas environment as well as within another inviscid liquid is very well examined theoretically and experimentally [1-10]. The transition point between the dripping and the laminar jetting point in gas environment or in a low viscous liquid is characterized by

$$We = \frac{\rho_D \cdot u_D^2 \cdot d_{c,i}}{\gamma} \geq 2 \qquad (1)$$

where ρ_D is the density, u_D the velocity of the disperse phase, γ the interfacial tension and $d_{c,i}$ the diameter of the capillary [9]. However, this is not valid for viscous fluids. At small Reynolds numbers, due to higher viscosities, significantly smaller critical Weber numbers are observed for the transition [11].

Meister and Scheele [10] presented an equation for the velocity u_J of the disperse phase for the first appearing jetting for low viscous liquids which is based on a force balance.

$$u_{jetting} = 1.73 \sqrt{\frac{\gamma}{\rho_D \cdot d_{c,i}} \left(1 - \frac{d_{c,i}}{d_{dripping}}\right)} \qquad (2)$$

This equation can only be solved iteratively, because $d_{dripping}$ is the droplet diameter which would form if jetting did not occur and can be calculated by equation (3). Equation (2) is valid for viscosities < 50 mPas. At higher viscosities the deviation to the experimental data increases [10]. For viscous liquids injected into viscous immiscible liquids a characteristic parameter or equation is still missing [8].

DRIPPING

Many equations and models have been presented for the prediction of the droplet diameter d_d or volume V_d, respectively in the dripping mode. Some of these are empirical and only valid for the variables investigated by the authors. Most of them have been obtained for low viscous liquids. In this range the equation given by Meister and Scheele [12], considering the buoyancy, interfacial tension, Stokes' drag and kinetic forces as well as the volume added during necking in their force balance, appears the best compromise between accuracy and ease of use for the dripping mode [13].

$$V_d = F\left[\frac{\pi \cdot \gamma \cdot d_{c,i}}{g \cdot \Delta\rho} + \frac{20 \cdot \mu_C \cdot \dot{V}_D}{d_d^2 \cdot g \cdot \Delta\rho} - \frac{4 \cdot \rho_D \cdot \dot{V}_D \cdot u_D}{3 \cdot g \cdot \Delta\rho}\right] + 4.5 \cdot F \cdot \sqrt[3]{\frac{\dot{V}_D^2 \cdot d_{c,i} \cdot \rho_D \cdot \gamma}{(g \cdot \Delta\rho)^2}} \qquad (3)$$

The Harkins-Brown correction factor F depends on the nozzle diameter $d_{c,i}$ and the drop volume V_d. $\Delta\rho$ is the density difference, μ_C the viscosity of the continuous phase and $\dot{V}_D$ the volumetric flow rate of the disperse phase.

Cramer [8] has investigated the influence of the flow conditions and the material properties of the two phases, particularly the interfacial tension experimentally. Higher velocities of the continuous phase and smaller interfacial tension lead to smaller droplets in the dripping mode. The experiments were done with liquids in a viscosity range of $0.001 < \mu < 0.244$ and a minimum density difference of $\Delta\rho = 81$ kg/m³.

JETTING

The drop formation in the laminar jetting regime was first investigated in gas environment by neglecting the surrounding fluid. Rayleigh [1, 2] observed that disturbances with a wavelength $\lambda_{R,crit}$ bigger than circumference of the jet with the diameter d_J leads to the break up.

$$\lambda_{R,crit} = \pi \cdot d_J \qquad (4)$$

In Tomotika's stability analysis a viscous liquid cylinder in stagnant viscous surrounding liquid is analysed theoretically. Tomotika found that the critical wavelength depends on the viscosity ratio of disperse to continuous phase $\alpha = \mu_D/\mu_C$. The maximum instability is observed at a viscosity ratio of $\alpha = 0.28$ and a corresponding wavelength of $\lambda_{crit} = 5.33\ d_J$ [14]. In this paper a viscosity ratio of $\alpha = 1$ is investigated for viscosities up to 1 Pas. The critical wavelength according to Tomotika is $\lambda_{crit} = 5.63\ d_J$ for this case [14].

The volume between two minima of the jet disturbance forms a droplet. The distance between these minima is the breakup wavelength λ_B. The resulting drop diameter d_d can be calculated by

$$d_d = \sqrt[3]{1.5 \cdot d_J^2 \cdot \lambda_B} \qquad (5)$$

where d_J is the diameter of the liquid jet. For the case of equal viscosities the droplet diameter is approximately twice the jet diameter [15].

In a co-flowing pipe flow the liquid jet expands or contracts after a short relaxation length directly after leaving the capillary. Neglecting the deformations due to capillary instabilities the resulting diameter and the contour of the jet depend on the volumetric flow rate ratio at given channel width [15].

For laminar flow the jet diameter in a tube after relaxation within the co-moving continuous phase can be calculated by assuming a parabolic velocity profile and no density difference. Further equal shear stress and equal velocities of both phases at the phase interface are implied independent of capillary effects. The further termed theoretical jet diameter *d'* is then described by equation (6) and equation (7) [15].

$$d' = D\sqrt{K - \sqrt{K^2 - K\varphi}} \tag{6}$$

$$K = \frac{\alpha}{\varphi - \alpha\varphi + 2\alpha - 1} \tag{7}$$

D is the tube diameter and φ the volumetric disperse phase fraction. The parameter K depends on the viscosity ratio $\alpha = \mu_D/\mu_C$ and the disperse phase fraction φ, too. The theoretical jet diameter depends only on the volumetric flow rate ratio of the phases and the viscosity ratio and it is independent on the capillary diameter. For the special case of equal viscosities equation (6) simplifies to equation (8) [15].

$$d' = D\sqrt{1 - \sqrt{1 - \varphi}} \tag{8}$$

In this paper the equation (6) can be evaluated via experimental data.

EXPERIMENTAL SETUP

The experimental setup is shown in Figure 2. The disperse phase is injected into the co-flowing continuous phase through a capillary. Both phases are tempered in their receiver tanks, because the viscosity has a large temperature dependency and so it can be guaranteed that the viscosity is constant and the experimental results are comparable and repeatable. The fluids were pumped with calibrated gear and syringe pumps to the channel and the capillary, respectively. The inner diameter of the capillary is $d_{c,i} = 3$ mm and the outer diameter is $d_{c,o} = 6$ mm. The capillary is sharpened at the end to obtain a smooth flow transition. The channel has a height of $H = 700$ mm and a quadratic cross-flow area of a x $a = 30$ x 30 mm², so an optical access, practicable without distortion is achieved. The mass-flow close to the edges of the channel is negligible, because the liquid fraction in laminar flow is less than 5 % of the total flow rate and the hydraulic diameter is equal to that of a cylinder with the same diameter as the channel edge length. The discharged fluid is collected and is separated for further use.

Pictures and videos are taken for analysing the drop formation with a digital camera (Fujifilm Finepix HS10) in HD quality or with a high-speed camera (Highspeedstar3, LaVision) with maximum numbers of pixels of 1024 x 1024. The videos are taken with a recording rate of 29 fps with the digital camera and 500 – 1000 fps with the high-speed camera. The illumination unit consists of eight Luxeon-LEDs to provide enough brightness at an exposure time of 2 ms.

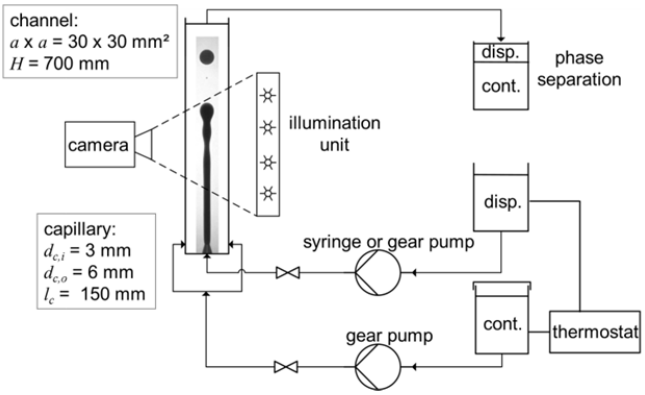

Figure 2 Scheme of experimental setup

The analysis is done by a self-written Matlab®-code. The break up length, the droplet diameter and the frequency of droplet formation are determined for the dripping regime. In the jetting regime the growth rate of the disturbance amplitude and the thread diameter and contour is also listed.

For the experiments with equal density the polyvinylpyrrolidone Luvitec K90 powder (BASF) is dissolved in water. The favoured viscosity of 1 Pas is adjusted and then the density is measured to 1024.9 kg/m³. A mixture of the silicone oils Tegiloxan 1000 (Evonik Goldschmidt GmbH) and silicon oil 12500 (Chemische Produkte D. Wilde) and brombenzene (Roth GmbH) is mixed to achieve the same density and viscosity as the continuous phase and is used as disperse phase. The disperse phase is coloured with "Sudanblau" II (Fluka) to differentiate the two phases. Both liquids show Newtonian flow behaviour at the given low shear-conditions. The interfacial tension between the two phases is $\gamma = 31.37$ mN/m.

Test series for constant theoretical jet diameter $d' = 2$, 3, 4 and 6 mm are performed by increasing the volumetric flow rates of both phases. At a theoretical jet diameter equal to the capillary diameter $d' = d_{c,i} = 3$ mm the velocities of both phases are equal.

RESULTS

During the experiments different phenomena could be observed. In the dripping regime as expected regular formed drops are detached with equal sizes. During the detachment a satellite drop is formed from the thin thread between droplet and capillary, as can be seen in Figure 3.

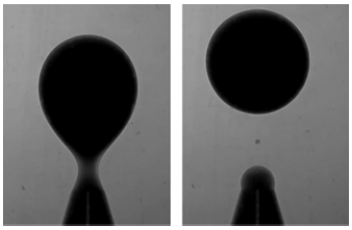

Figure 3 Dripping with satellite drop

In the jetting regime different kinds of droplet formation could be identified when the magnitude of the flow velocity of both phases is about the same. In Figure 4 typical phenomena are presented. In A regular jetting is shown. Satellite droplets are formed as in the dripping mode, but in the jetting regime the satellite droplets are bigger and sometimes more than one satellite occurs. In B the thread is retired and merges again with the jet. A common drop formation is the generation of so-called double droplets (C, D). Droplets results normally from each wave on the jet surface. Double droplets form a drop from two surface waves. The second disturbance has a bigger growth rate than the first one and pushes the liquid into the first droplet. A droplet with double volume is developed. The two waves coalesce before (C) or after (D) the break up. If a part of the jet breaks up of the original jet and then disintegrates into droplets it is called bar-bell droplets and can be seen in E.

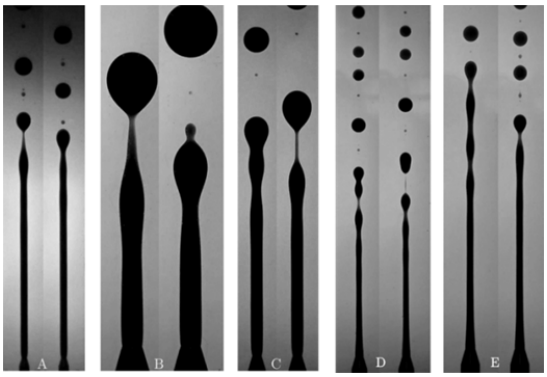

Figure 4 Different drop formation phenomena in the jetting regime; A: regular jetting with satellite drops, B: satellite drops merges with thread, C, D: formation of a double droplet and E: formation of bar-bell droplet

TRANSITION BETWEEN DRIPPING AND JETTING

The distance between the generated droplets in the upper part of the channel is a sensitive parameter to obtain the transition point between dripping and jetting. In the jetting region this distance refers to the breakup wavelength λ_B. In Figure 5 the breakup wavelength related to the Rayleigh wavelength $\lambda_{R,crit} = \pi d'$ [1, 2] is plotted against the capillary number Ca, which is calculated by equation (9) with the mean discharge velocity u_D and viscosity μ_D of the disperse phase and the interfacial tension γ.

$$Ca = \frac{u_D \cdot \mu_D}{\gamma} \qquad (9)$$

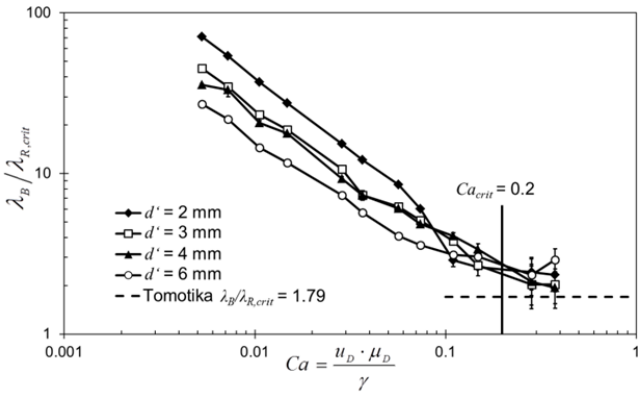

Figure 5 Determination of the transition point between dripping and jetting via the break up wavelength or the distance between the droplets resp.

The presented results show the experiments of constant theoretical jet diameter d'. At low capillary numbers the distance between the droplets is large and it decreases with increasing capillary number. At a capillary number of around $Ca = 0.2$ a value of $\lambda_B / \lambda_{R,crit} = 2.145 \pm 0.2$ is reached and remains constant. The transition point between dripping and jetting mode always occurs at the same capillary number Ca. Neither a contraction ($d' = 2$ mm) nor an expansion ($d' = 4$, 6 mm) has any influence of the transition point. For equal densities and viscosities a critical capillary number Ca_{crit} is observed at

$$Ca_{crit} = \frac{u_D \cdot \mu_D}{\gamma} = 0.2 \,. \qquad (10)$$

The constant value of $\lambda_B / \lambda_{R,crit}$ lies insignificantly above the limited value of the wavelength given by Tomotika [14] of $\lambda_B / \lambda_{R,crit} = 1.79$ for this case. The wavelength in this system can then be expressed by equation (11).

$$\lambda_B = 6.74 \cdot d' \qquad (11)$$

The standard deviation of the experimental data is also shown in Figure 5 and it can be observed that with passing the transition point the standard deviation increases according to different phenomena arising at given flow data as in figure 4.

DROPLET DIAMETER

The droplet diameter depends on the drop formation regime. In Figure 6 the measured droplet sizes are related to capillary diameter $d_{c,i}$ and plotted against the capillary number $Ca = u' \mu_D / \gamma$. In this case the capillary number is calculated by the velocity at the phase interface u', this means the velocity at $d'/2$ from the centre of the channel.

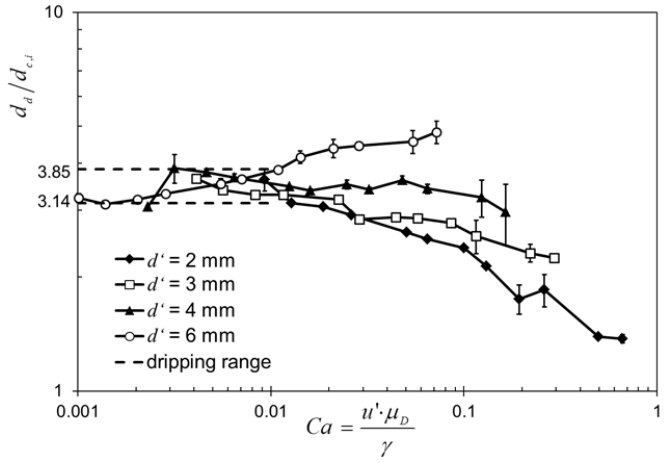

Figure 6 Droplet diameter related to the capillary diameter vs the capillary number for different theoretical jet diameters

At small capillary numbers the measurement points fall together, whilst at higher capillary numbers the lines disperse. The relationship between the droplet diameter and the capillary diameter can be described by equation (12) for these experiments.

$$d_{d,dripping} = 3.5 \cdot d_{c,i} \quad (12)$$

In Figure 7 the experimental results of the droplet diameter are related to the theoretical jet diameter *d'*. In this plot the behaviour is inverse. In the jetting regime referring to higher capillary numbers, the points are in the same range whereas in the dripping mode at lower capillary numbers the points are scattered.

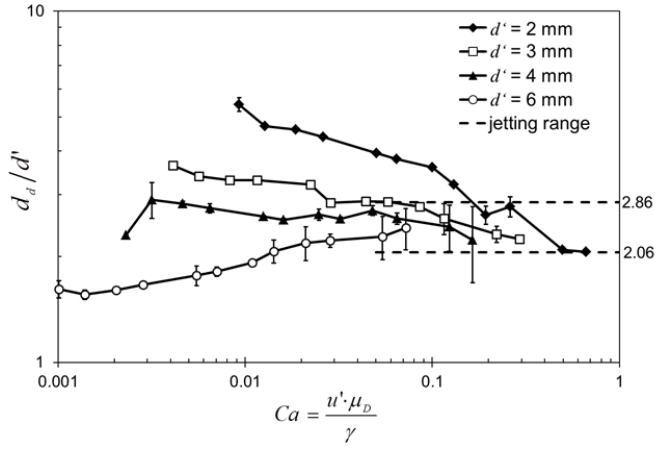

Figure 7 Droplet diameter related to the theoretical jet diameter against the capillary number for different theoretical jet diameters

Equation (13) shows the relation between droplet diameter $d_{d,jetting}$ and the theoretical jet diameter *d'*.

$$d_{d,jetting} = 2.46 \cdot d' \quad (13)$$

According to the determined breakup wavelength in equation (11) and the relationship between the wavelength and the droplet diameter (equation (5)) the droplet diameter in the jetting regime can be calculated by

$$d_{d,jetting} = 2.162 \cdot d' \quad (14)$$

The deviation between equation (13) and equation (14) can be explained by the different drop formation phenomena described earlier. The average droplet diameter of the measured drops is larger because of the generation of double droplets that are also included in the experimental results. The different droplet formation phenomena are the consequence of disturbances, with different wavelength and different growth rates above the critical wavelength, see Figure 5.

JET DIAMETER

The test series with constant theoretical jet diameter are chosen to investigate a contraction of the jet at *d'* = 2 mm and expansions of the jet for *d'* = 4 and 6 mm. Furthermore a test series is performed with a theoretical jet diameter equalling the capillary diameter $d' = d_{c,i} = 3$ mm. In Figure 8 pictures of the generated jets are shown. It can be seen that both contraction for $d' < d_{c,i}$ and expansion for $d' > d_{c,I}$ occur.

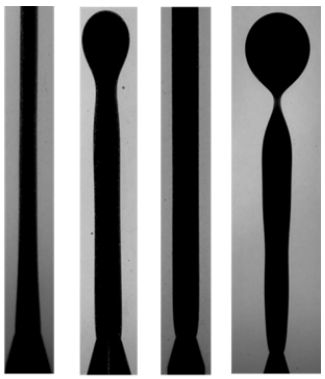

Figure 8 Pictures of jets generated for different theoretical jet diameters

In Figure 9 the deviation of the theoretical jet diameter *d'* from the real jet diameter d_J is presented. The real jet diameter d_J related to the capillary diameter is plotted against the theoretical jet diameter d' also related to the capillary diameter.

All measured jet diameters are in the range of ± 20 % of relative deviation. The only negative deviation is for the theoretical jet diameter of *d'* = 6 mm. In Figure 8 disturbances on the jet surface can be seen before the jet reaches its maximum diameter. The widening of the jet obviously triggers growth of waves.

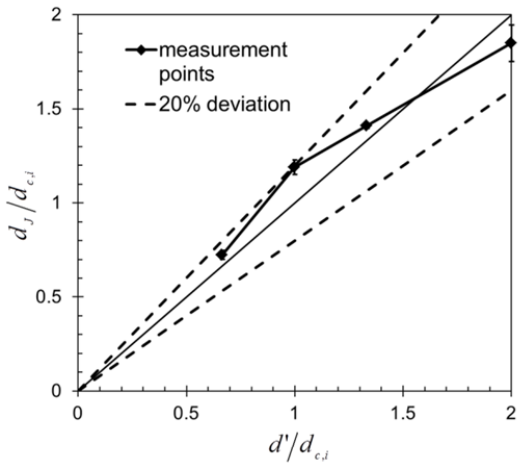

Figure 9 Deviation between calculated and experimentally measured jet diameters

In Figure 10 the relaxation length $L_{Relaxation}$ for the different theoretical jet diameter except for $d' = 6$ mm are shown. The relaxations length is defined as the distance from the capillary to the point where a cylindrical jet is reached and contraction or expansion has ceased. In the diagram the relaxation length and the theoretical jet diameter are related to the capillary diameter.

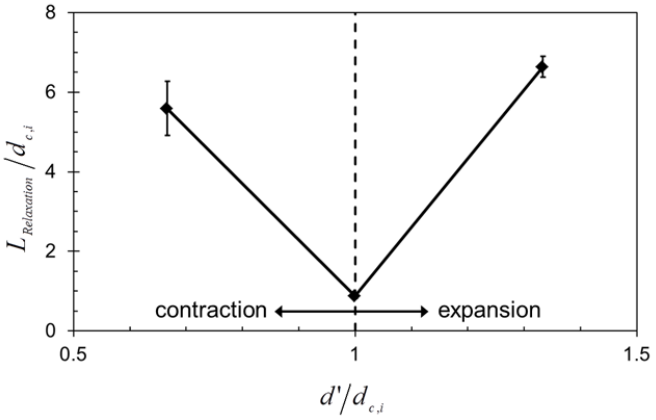

Figure 10 Relaxation length for different theoretical jet diameter

At equal theoretical jet diameter and capillary diameter the relaxation length is at its minimum, neither a contraction nor an expansion is expected. If the jet contracts or expands only 1 mm, the relaxation length here is around 6 times the capillary diameter.

CONCLUSION

A viscous liquid-liquid-system is investigated experimentally for equal density $\rho = 1024.9$ kg/m³ and equal viscosity $\mu = 1$ Pas. The transition between dripping and laminar jetting is observed at critical capillary number of $Ca = 0.2$ independent of the volumetric flow rate ratio or the theoretical jet diameter, respectively. In the jetting regime different kinds of drop formation phenomena are noticed: satellite, double and bar-bell droplets. The determined breakup wavelength are found slightly above the critical wavelength of Tomotika [14] and have a broad standard deviation which is correlated to different types of drop formation. Nevertheless the comparison with literature data considering the complexity of the real breakup is quite well. The relationship between breakup wavelength and droplet size for the prediction of the droplet sizes in the jetting regime could be confirmed as well.

As a consequence it must be stated that equal sized droplet even though formed in the "low flow rate" dripping regime cannot be expected in any case when jetting is applied and the liquids are viscous.

Thanks to the **DFG** for the financial support of the project within the Paketantrag 187 „Modellgestützte Entwicklung fluider Prozesse mit disperser Phase".

REFERENCES

[1] Rayleigh, J.W.S., On the Instability of Jets, *Proceedings of the London Mathematical Society,* Vol. 10, 1878, pp. 4-13

[2] Rayleigh, J.W.S., On the Capillary Phenomena of Jets, *Proceedings of the Royal Society of London,* Vol. 29, 1879, pp. 71-97

[3] Weber, C., Zum Zerfall eines Flüssigkeitsstrahles, *Zeitschrift für Angewandte Mathematik und Mechanik,* Vol. 11, No. 2, 2031, pp. 136-154

[4] Meister, B.J., and Scheele, G.F., Prediction of Jet Length in Immiscible Liquid Systems, *AIChE Journal,* Vol. 15, No. 5, 1969, pp. 689-699

[5] Meister, B.J., and Scheele, G.F., Drop Formation from Cylindrical Jets in Immiscible Liquid Systems, *AIChE Journal,* Vol. 15, No. 5, 1969, pp. 700-706

[6] Kitamura, Y., Mishima, H., and Takahashi, T., Stability of Jets in Liquid-Liquid-Systems, *The Canadian Journal of Chemical Engineering,* Vol. 60, No. 6, 1982, pp. 723-731

[7] Homma, S., et al, Breakup Mode of an Axisymmetric Liquid Jet Injected into Another Immiscible Liquid, *Chemical Engineering Science,* Vol. 61, No. 12, 2006, pp. 3986-3996

[8] Cramer, C., Fischer, P., and Windhab, E.J.,Drop Formation in a Co-Flowing Ambient Fluid, *Chemical Engineering Science,* Vol. 59, No. 15, 2004, pp. 3045-3058

[9] Ruff, K., Tropfengröße beim Strahlzerfall in niedrigviskosen Flüssig/Flüssig-Systemen, *Chemie Ingenieur Technik,* Vol. 50, No. 6, 1978, pp. 441-444

[10] Scheele, G.F., and Meister, B.J., Drop Formation at Low Velocities in Liquid-Liquid-Systems: Part II. Prediction of Jetting Velocity, *AIChE Journal,* Vol. 14, No. 1, 1968, pp. 15-19

[11] Leib, S.J., and Goldstein, M.E., Convective and Absolute Instability of a Viscous Liquid Jet, *Physics of Fluids,* Vol. 29, No. 4, 1986, pp. 952-954

[12] Scheele, G.F., and Meister, B.J., Drop Formation at Low Velocities in Liquid-Liquid-Systems: Part I. Prediction of Drop Volume, *AIChE Journal,* Vol. 14, No. 1, 1968, pp. 9-14

[13] Clift, R., Grace, J.R., and Weber, M.E., Bubbles, Drops and Particles, *Dover Publicationy, New York,* 2005

[14] Tomotika, S., On the Instability of a Cylindrical Thread of a Viscous Liquid Surrounded by Another Viscous Fluid, *Proceedings of the Royal Society of London. Series A, Mathematical and Physical Sciences,* Vol. 150, No. 870, 1935, pp. 322-337

[15] Sellerberg, M., and Walzel, P., Behavior of Elongated liquid Jets in Viscous Liquid-Liquid-Sytems, *Chemical Engineering & Technology,*Vol. 34, No. 12, 2011, pp. 2099-2104